The Astrophysical Journal Letters, 958:L17 (8pp), 2023 November 20 https://doi.org/10.3847/2041-8213/ad0887

PSR J2150+3427: A Possible Double Neutron Star System

Q. D. Wu[1,2,3,4], N. Wang[1,3,4], J. P. Yuan[1,3,4], D. Li[1,5,6], P. Wang[5,7], M. Y. Xue[5], W. W. Zhu[5,7], C. C. Miao[8], W. M. Yan[1,3,4], J. B. Wang[1,3,9], J. M. Yao[1,3,4], S. Q. Wang[1,3,4], S. N. Sun[1,3,4], F. F. Kou[1,3,4], D. Zhao[1,3,4,10], Y. T. Chen[2,5], S. J. Dang[11], Y. Feng[8], Z. J. Liu[11], X. L. Miao[5], L. Q. Meng[5], M. Yuan[5], C. H. Niu[5,12], J. R. Niu[5], L. Qian[5], S. Wang[13], X. Y. Xie[11], Y. F. Xiao[14], Y. L. Yue[5], S. P. You[11], X. H. Yu[11], R. S. Zhao[11], R. Yuen[1,3,4], X. Zhou[1,3,4], and L. Zhang[5]

[1] Xinjiang Astronomical Observatory, Chinese Academy of Sciences, 150 Science 1-Street, Urumqi, Xinjiang 830011, People's Republic of China; na.wang@xao.ac.cn, yuanjp@xao.ac.cn, dili@nao.cas.cn
[2] University of Chinese Academy of Sciences, Beijing 100049, People's Republic of China
[3] Key Laboratory of Radio Astronomy, Chinese Academy of Sciences, Urumqi, Xinjiang 830011, People's Republic of China
[4] Xinjiang Key Laboratory of Radio Astrophysics, 150 Science1-Street, Urumqi, Xinjiang 830011, People's Republic of China
[5] National Astronomical Observatories, Chinese Academy of Sciences, A20 Datun Road, Chaoyang District, Beijing 100101, People's Republic of China
[6] NAOC-UKZN Computational Astrophysics Centre, University of KwaZulu-Natal, Durban 4000, South Africa
[7] Institute for Frontiers in Astronomy and Astrophysics, Beijing Normal University, Beijing 102206, People's Republic of China
[8] Zhejiang Lab, Hangzhou, Zhejiang 311121, People's Republic of China
[9] Institute of Optoelectronic Technology, Lishui University, Lishui, 323000, People's Republic of China
[10] Department of Physics, Xinjiang University, 830046, Urumqi, People's Republic of China
[11] Guizhou Normal University, Guiyang 550001, People's Republic of China
[12] Institute of Astrophysics, Central China Normal University, Wuhan 430079, People's Republic of China
[13] School of Computer Science, Fudan University, Shanghai 200438, People's Republic of China
[14] GuiZhou University, Guizhou 550025, People's Republic of China
Received 2023 July 8; revised 2023 October 30; accepted 2023 October 30; published 2023 November 21

Abstract

PSR J2150+3427 is a 0.654 s pulsar discovered by the Commensal Radio Astronomy FAST Survey. From the follow-up observations, we find that the pulsar is in a highly eccentric orbit ($e = 0.601$) with an orbital period of 10.592 days and a projected semimajor axis of 25.488 lt-s. Using 2.7 yr of timing data, we also measured the rate of periastron advance $\dot{\omega} = 0.0115(4)$ deg yr^{-1}. An estimate for the total mass of the system using the $\dot{\omega}$ gives $M_{\rm tot} = 2.59(13) M_{\odot}$, which is consistent with most of the known double neutron star (DNS) systems and one neutron star (NS)–white dwarf (WD) system named B2303+46. Combining $\dot{\omega}$ with the mass function of the system gives the masses of $M_p < 1.67$ and $M_c > 0.98\,M_{\odot}$ for the pulsar and the companion star, respectively. This constraint, along with the spin period and orbital parameters, suggests that it is possibly a DNS system, and we cannot entirely rule out the possibility of an NS–WD system. Future timing observations will vastly improve the uncertainty in $\dot{\omega}$, and are likely to allow the detection of additional relativistic effects, which can be used to modify the values of M_p and M_c. With a spin-down luminosity of $\dot{E} = 5.07(6) \times 10^{29}$ erg s^{-1}, PSR J2150+3427 is a very low-luminosity pulsar, with only the binary pulsar J2208+4610 having a smaller $\dot{E}$.

Unified Astronomy Thesaurus concepts: Binary pulsars (153); Pulsars (1306); Radio pulsars (1353); Neutron stars (1108)

1. Introduction

The Five-hundred-meter Aperture Spherical radio Telescope (FAST) is an ideal telescope for discovering pulsars (Nan et al. 2011; Qian et al. 2020). Pulsar searching is a key aspect of the Commensal Radio Astronomy FAST Survey (CRAFTS; Li et al. 2018), which samples the sky area between the range of $-14° <$ decl. $<66°$ in drift-scan mode (Cruces et al. 2021) using the FAST 19-beam receiver with a total bandwidth of 1.05–1.45 GHz and a center frequency of 1.25 GHz (Jiang et al. 2020). Currently, the CRAFTS survey has discovered about 179 new pulsars,[15] 57 of which have their timing solutions reported from earlier studies (Cameron et al. 2020; Cruces et al. 2021; Miao et al. 2023; Wu et al. 2023).

About 11% of the known pulsars are in binary systems (ATNF Pulsar Catalogue v1.69; Manchester et al. 2005), with the majority (∼84%) being millisecond pulsars (MSPs) with spin period $P < 20$ ms. MSPs are proposed to be formed from the evolution of low-mass X-ray binaries (Bhattacharya & van den Heuvel 1991). In the evolutionary scenario known as the "recycling" process (Alpar et al. 1982; Bhattacharya et al. 1992), the neutron star (NS) gains angular momentum from its companion via the Roche lobe overflow and spins up to millisecond periods. The outcome of the process is typically an MSP with a helium white dwarf (WD) companion in an extremely circular ($e < 10^{-3}$) orbit (Phinney 1992).

Some rare binary pulsars may experience a different evolutionary path. In the case when the companion star is massive enough to evolve into a supernova explosion, and the binary system is not disrupted by the explosion, a double neutron star (DNS) system will be formed. In such a system, the firstborn pulsar is a recycled pulsar, and the second-born NS will have the spin characteristics consistent with that of canonical pulsars (Agazie et al. 2021). Currently, 20

[15] http://groups.bao.ac.cn/ism/CRAFTS/

confirmed and 9 candidate DNS systems have been published[16] (Özel & Freire 2016). They have orbital periods between $0.078 \leqslant P_b \leqslant 45.06$ days and eccentricity of $0.064 \leqslant e \leqslant 0.83$. The spin periods of the recycled pulsars in DNS systems range from 16 to 186 ms, the period derivatives from 2.72×10^{-20} to 1.80×10^{-17} s s^{-1}, and the inferred magnetic field strength between 1×10^9 G and 6×10^{10} G (Manchester et al. 2005; Pol et al. 2019; Agazie et al. 2021).

For the nonrecycled (younger) pulsars in DNS systems (for example PSRs J1906+0746, J1755−2550, and J0737−3039B), their spin periods are found between $144 \leqslant P \leqslant 2770$ ms. They also possess greater magnetic field strengths ($\sim 8.86 \times 10^{11}$–1.73×10^{12} G) and higher period derivatives ($\sim 8.92 \times 10^{-16}$–$2.03 \times 10^{-14}$ s s^{-1}). At present, PSR J0737−3039A/B system is the only known double pulsar system (Özel & Freire 2016; Kramer et al. 2021).

The evolution of a DNS system and its progenitor plays an important role in many fields of astrophysics, including powerful gravitational wave emission (Wex 2014), modeling of X-ray binary accretion processes, formation of millisecond pulsars (Lewin & van der Klis 2006), and possibly gamma-ray bursts (Eichler et al. 1989; Cantiello et al. 2007). In addition, the ancestors of the detected DNS systems experienced multiple mass transfer stages, with one or more common envelope episodes, and two supernova explosions, which make their observed characteristics similar to fossil records that have stored their past evolutionary history (Tauris & van den Heuvel 2006; Tauris et al. 2017). Therefore, DNS systems can be used as key probes in binary stellar astrophysics. Furthermore, some DNSs in relativistic orbits are ultrastable clocks, allowing unprecedented testing of gravitational theory in strong field states (Wex 2014). Finally, DNS systems help to constrain the equation of state of nuclear matter in high density (Özel & Freire 2016).

In this paper, we report the discovery and properties of PSR J2150+3427 based on FAST observations. It is a binary pulsar in a 10 day ($P_b \sim 10.592$ days) orbit with eccentricity $e \sim 0.601$ and a spin period $P \sim 654$ ms. Examination of the orbital period, eccentricity, companion mass (M_c), and the total mass of system ($M_{\rm tot}$) suggests that this system is likely a DNS system.

2. Observations and Analysis

PSR J2150+3427 was discovered in an observation conducted on 2019 October 30, and confirmed in a drift scan using an *L*-band 19-beam receiver (see CRAFTS pulsar list). Our observations were performed at 91 different epochs between 2020 December and 2023 April using the FAST 19-beam receiver at a center frequency of 1250 MHz and a bandwidth of 400 MHz (Jiang et al. 2020). The duration for most observations is 12 minutes, while three dozen epochs have a duration of 4 minutes and only one observation has an integration time of 30 minutes. A polarization calibration signal generated by a noise diode was recorded for 40 s before each pulsar observation. After the polarimetric calibration, the tool `rmfit` in the `PSRCHIVE`[17] software package (Hotan et al. 2004; van Straten et al. 2011) was used to search for the Faraday rotation measure (RM). The polarization profile shown in Figure 1 is obtained from the observation with the highest signal-to-noise ratio.

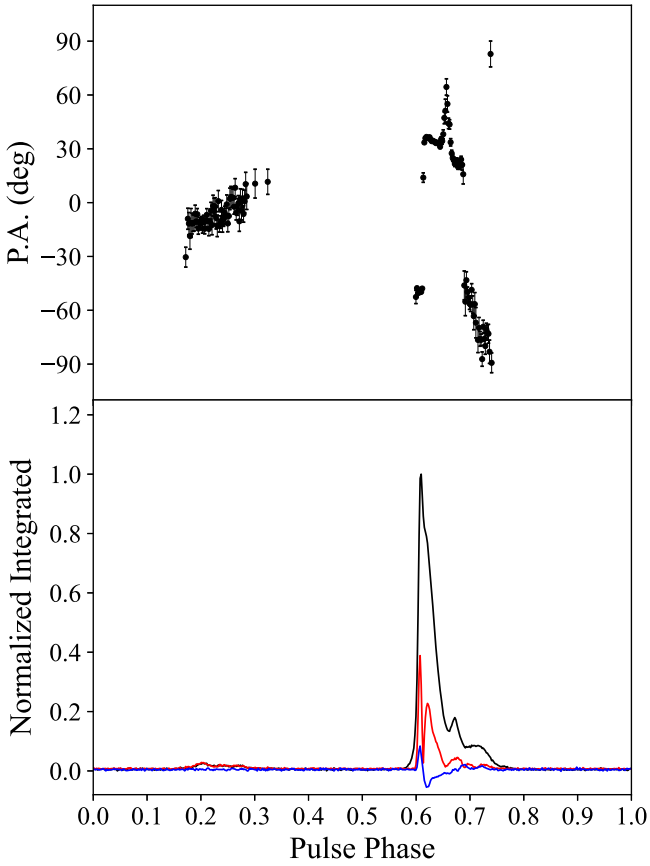

Figure 1. Integrated polarization profiles of PSR J2150+3427. In the upper panel, the black dots with error bars are the PA points. The total intensity, linearly polarized flux and the circular-polarized flux are shown in black, red, and blue, respectively, in the lower panel.

We dedispersed and folded the data using the DSPSR[18] (van Straten & Bailes 2011). The radio frequency interference (RFI) was excised using the `pazi` and `paz` tools in the `PSRCHIVE`. It was then followed by adding all the phase-aligned profiles using the `psradd` tool. The `pat` tool from `PSRCHIVE` was used to compute the times of arrival (TOAs). The `paas` tool was used to generate a standard profile, which was then used to calculate the TOAs to refine the timing ephemeris. Finally, the `TEMPO2`[19] (Edwards et al. 2006; Hobbs et al. 2006) was used to build a phase-connected timing solution.

3. Results

3.1. Preliminary Orbital Analysis

Since timing analysis requires initial estimates of the Kepler binary parameters, we first measure the barycenter spin period $P_{\rm obs}$ for every observation using the `TEMPO2` package. After that, a series of $P_{\rm obs}$ is fitted using the `fitorbit`[20] program in order to derive the first-order orbital parameters. As shown in panel (a) of Figure 2, the measured $P_{\rm obs}$ between MJD 59700 and MJD 59729 reveals a 10.592 day orbit with an eccentricity of $e = 0.601$.

[16] https://www3.mpifr-bonn.mpg.de/staff/pfreire/NS_masses.html
[17] http://psrchive.sourceforge.net/
[18] https://dspsr.sourceforge.net/
[19] https://www.atnf.csiro.au/research/pulsar/tempo2
[20] https://github.com/vivekvenkris/fitorbit

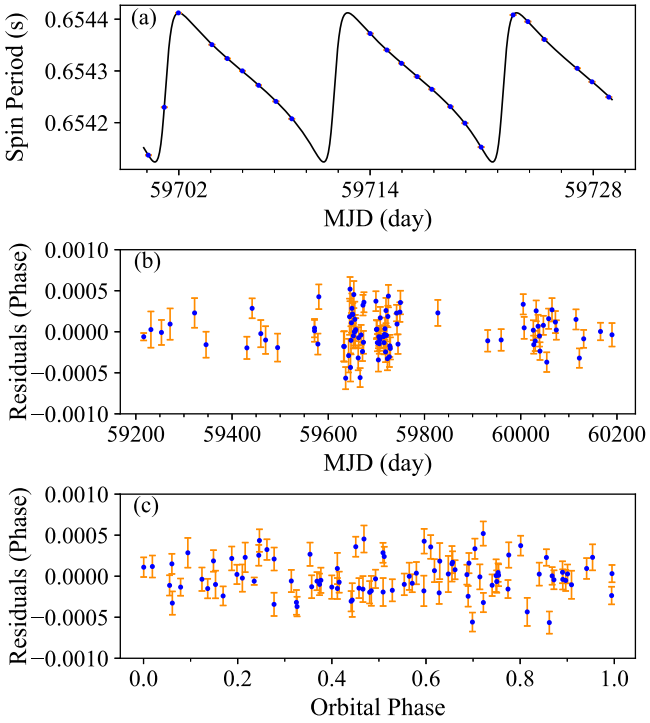

Figure 2. Panel (a): the observed Doppler-modulated spin period (P) vs. MJD. It clearly shows that the pulsar orbit has a significant eccentricity. The black line is a best-fit orbital model obtained using $P_b \sim 10.592$ (day), $x_p \sim 25.488$ (lt-s), $e \sim 0.601$, $T_0 \sim 59626.993$ (MJD), and $\omega \sim 262.791$ (deg). Panels (b) and (c) show plots for postfit residuals vs., respectively, the MJD and orbital phase for 92 TOAs over 91 epochs.

3.2. Pulsar Timing

In this section, we outline the steps for improving the orbital ephemeris derived in Section 3.1 through a process known as pulsar timing. For observations with integration time of either 4 or 12 minutes, we calculated one TOA for each epoch, whereas two TOAs were produced for the observation with an integration time of 30 minutes. We fitted the dispersion measure (DM) by dividing the bandwidth into two frequency subbands and the TOA was calculated separately for each subband. A reduced $\chi^2 \sim 1$ was obtained by combining a scaling factor applied to all raw TOA uncertainties (called EFAC), and adding a term in quadrature to the TOA uncertainties (called EQUAD).

Our total data set spanned roughly 2.7 yr (MJD 59216–60189). The resulted ephemeris and timing residuals are shown in Table 1 and Figure 2, respectively. Apart from the least-squares method, the Bayesian timing analysis is also conducted using `TEMPONEST` (Lentati et al. 2014), and both return consistent results. In Table 1 the ephemeris is reported in barycentric coordination time (TCB) units, which is derived from the Damour & Deruelle's (DD) binary model (Damour & Deruelle 1985, 1986) and the JPL DE438[21] solar system ephemeris. The rms of our timing solution is 147.086 μs.

From the measured orbital period (P_b) and the projected semimajor axis of orbit (x), we obtain the mass function

$$f(M_p, M_c) = \frac{(M_c \sin i)^3}{M_{\rm tot}^2} = \frac{4\pi^2}{T_\odot}\frac{x^3}{P_b^2} = 0.158(4) M_\odot, \quad (1)$$

[21] ftp://ssd.jpl.nasa.gov/pub/eph/planets/bsp/de438.bsp

Table 1
Timing Solution for PSR J2150+3427

Statistic and Model Parameters	Value
Timing data span (MJD)	59216–60189
Reference epoch (MJD)	59474
Solar system ephemeris	DE438
EFAC	2.1
EQUAD (μs)	9
Number of TOAs	93
rms residual (μs)	147.086
Measured Parameter	**Value**
R.A., α (J2000)	21:50:33.007(1)
decl., δ (J2000)	+34:27:37.31(2)
Proper motion in α, μ_α (mas yr^{-1})	−51(25)
Proper motion in δ, μ_δ (mas yr^{-1})	−46(24)
Spin frequency, ν (s^{-1})	1.528397635626(3)
Spin frequency derivative, $\dot{\nu}$ (s^{-2})	$-8.4(1)\times10^{-18}$
Dispersion measure (pc cm^{-3})	55.48(3)
Faraday rotation measure (rad m^{-2})	97.4(1)
Binary Parameters	**Value**
Binary model	DD
Orbital period, P_b (days)	10.5921329(3)
Epoch of periastron, T_0 (MJD)	59626.993390(7)
Projected semimajor axis, x (lt-s)	25.48802(3)
Longitude of periastron, ω (deg)	262.7911(3)
Orbital eccentricity, e	0.601494(2)
Advance of periastron, $\dot{\omega}$ (deg yr^{-1})	0.0115(4)
Derived Parameters	**Value**
P (s)	0.654279996704(1)
$\dot{P}$ (s s^{-1})	$3.60(4)\times10^{-18}$
Characteristic age (Gyr)	2.88(3)
Surface magnetic field (10^{10} G)	4.90(2)
Spin-down luminosity (10^{29} erg s^{-1})	5.07(6)
Mass function ($M_\odot$)	0.158(4)
Minimum companion mass ($M_\odot$)	0.94
Median companion mass ($M_\odot$)	1.15
Total mass ($M_\odot$)	2.59(13)
Total proper motion, μ (mas yr^{-1})	69(25)
Dist$_{DM}$ YMW16 (kpc)	4.77
Dist$_{DM}$ NE2001 (kpc)	3.00
S_{1250} (mJy)	0.228(8)[a]

Notes. Timing results are obtained with tempo2 and reported in units of TCB.
[a] The flux density at 1.25 GHz was estimated using the radiometer equation from Lorimer & Kramer (2004).

where $M_{\rm tot} = M_p + M_c$ is the total mass of the system, M_c and M_p are masses for the companion and the pulsar, respectively, and i is the angle between the orbital angular momentum vector and the line of sight. The mass of the Sun in time units is given by $T_\odot = GM_\odot/c^3 = 4.925490947$ μs, G is the Newton's gravitational constant, $M_\odot$ is the mass of the Sun, and c is the speed of light. Assuming a system inclination of 90° (Lorimer 2008), the mass function given in Equation (1) implies a minimum companion mass of $M_c = 0.94$ $M_\odot$. The orbital eccentricity in the orbital solution allows us to measure one post-Kepler (PK) parameter, namely the periastron advance, which is estimated to be $\dot{\omega} = 0.0115(4)$ deg yr^{-1}. If $\dot{\omega}$ is purely relativistic, the total mass ($M_{\rm tot}$) of the binary system can be determined by the following equation

(Taylor & Weisberg 1982):

$$\dot{\omega} = 3\frac{T_{\odot}^{2/3}}{(1-e^2)}\left(\frac{P_b}{2\pi}\right)^{-5/3} M_{\rm tot}^{2/3}. \quad (2)$$

Using the measured $\dot{\omega}$ gives the total mass of the system $M_{\rm tot} = 2.59(13) M_{\odot}$, where the uncertainty is 1σ. The total mass is greater than the lightest DNS system, known as the PSR J1018−1523 ($M_{\rm tot} = 2.3(3)\ M_{\odot}$; Swiggum et al. 2023), but consistent with most confirmed DNSs (e.g., PSRs J0737−3039A/B, Kramer et al. 2021; J1208−5936, Bernadich et al. 2023; J1325−6253, Sengar et al. 2022; J1411+2551, Martinez et al. 2017; J1756−2251, Ferdman et al. 2014; J1811−1736, Corongiu et al. 2007), and more. The remaining PK parameters cannot be determined for this system at this stage, making it impossible to evaluate the individual mass in this binary. However, the pulsar and companion mass can be constrained with the constraint $\sin i \leqslant 1$ from the mass function (f). We obtain the lower limit for M_c, such that

$$M_c > \sqrt[3]{M_{tot}^2 f(M_p, M_c)} = 1.02(4) M_{\odot}. \quad (3)$$

Panel (a) of Figure 3 shows the "mass–mass" diagram, which demonstrates the possible pulsar and companion masses allowed by $\dot{\omega}$ and those forbidden by the mass function. We obtain $M_p < 1.67\ M_{\odot}$ and $M_c > 0.98\ M_{\odot}$ (1σ error) for the pulsar and the companion, respectively. In other confirmed DNS systems with total system mass measurements only, such as PSRs J1325−6253, J1411+2551, J1759+5036, and J1811−1736, a similar range for the companion masses to PSR J2150+3427 is observed.

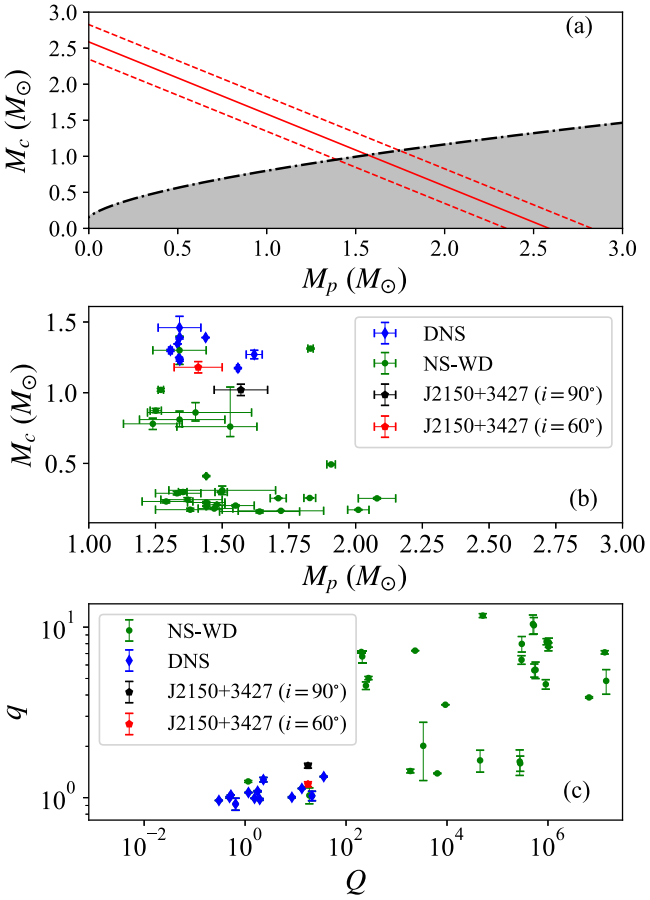

Figure 3. Panel (a): the mass–mass diagram of PSR J2150+3427 obtained from pulsar timing assuming fully general relativity. The gray region is excluded based on the mass function (black dotted line) and orbital geometry. The red line corresponds to $\dot{\omega} = 0.0115(4)$ deg yr^{-1}, and the dotted line shows the regions that are consistent within the error in $\dot{\omega}$. Panel (b): mass–mass diagram for known pulsars and PSR J2150+3427. Panel (c): the Q–q diagram of PSR J2150+3427 and the systems with the NS mass measured. Here, $q = M_p/M_c$ is the system mass ratio, and $Q = P_b/e$ (day) is the orbital factor. The blue diamonds are the DNS systems with individual NS mass measurements. The green dots are the NS–WD systems with individual NS mass measurements. The black and red stars of the PSR J2150+3427 system are calculated assuming the orbital inclination of $i = 90°$ and 60°, respectively.

4. Discussion

The spin period of PSR J2150+3427 is consistent with most canonical pulsars that have a period derivative as small as $\dot{P} = 3.60(4) \times 10^{-18}$ s s^{-1}. This gives the characteristic age of 2.88(3) Gyr and the surface magnetic field strength of $B_s = 4.90(2) \times 10^{10}$ G. The measured P and $\dot{P}$ imply that PSR J2150+3427 possesses a small spin-down luminosity of $\dot{E} = 5.07(6) \times 10^{29}$ erg s^{-1}, and only 12 pulsars in PSRCAT[22] (version 1.69) have smaller luminosity. The magnetic field strength and the small $\dot{P}$ suggest that PSR J2150+3427 may be slightly recycled. The high eccentricity is likely the aftermath of the supernova explosion of the companion star, which is consistent with the DNS systems showing high eccentricity (Tauris et al. 2017; Pol et al. 2019; Balakrishnan et al. 2023) and two NS–WD systems (Davies et al. 2002).

4.1. Intrinsic Spin-down Rate

In general, the observed spin-period derivative ($\dot{P}_{\rm obs}$) is given by

$$\begin{aligned}\frac{\dot{P}_{\rm obs}}{P} &= \frac{\dot{P}_{\rm int}}{P} + \frac{\dot{P}_{\rm shk}}{P} \\ &= \frac{\dot{P}_{\rm int}}{P} + \frac{V^2}{cd} \\ &= \frac{\dot{P}_{\rm int}}{P} + \frac{\mu^2 d}{c},\end{aligned} \quad (4)$$

where $\dot{P}_{\rm int}$ is the intrinsic spin-down rate, $\dot{P}_{\rm shk}$ is the Shklovskii correction to the period derivative $\dot{P}$, V is the transverse velocity, and d is the distance to the pulsar. The V^2/cd and $\mu^2 d/c$ are the so-called Shklovskii effect (Shklovskii 1970). Hence, $V = \mu d$ and $V < (\dot{P}_{\rm obs}/P)dc$. The determination of $\dot{P}_{\rm int}$ and V depends on reliable distances. According to the results by Deller et al. (2019) on the parallax distance for 57 pulsars, both electron density models (NE2001, Cordes & Lazio 2002; and YMW16, Yao et al. 2017) have significant shortcomings, especially in the high-latitude regions of the Galaxy. The Galactic latitude of PSR J2150+3427 is $b = -15.002$, and its DM distance may not be reliable.

At the DM distance derived from the NE2001 model (3 kpc), we obtain the upper transverse velocity limit of $V < 392(4)$ km s^{-1}, based on $V < (\dot{P}_{\rm obs}/P)dc$, and $\dot{P}_{\rm shk} < 3.63(8) \times 10^{-18}$ s s^{-1}. With the distance derived from the YMW16 model (4.77 kpc), $V < 495(5)$ km s^{-1}, and $\dot{P}_{\rm shk} < 3.63(8) \times 10^{-18}$ s s^{-1} are obtained. The maximum $\dot{P}_{\rm shk}$ obtained from both distances is greater than $\dot{P}_{\rm obs}$ ($3.62(7) \times 10^{-18}$ s s^{-1}). This

[22] https://www.atnf.csiro.au/research/pulsar/psrcat/

implies that the actual distance is possibly less than 3 kpc. Due to the lack of reliable distance, the reliable values of $\dot{P}_{\rm int}$ and V are not obtained.

4.2. System Origin

Comparing PSR J2150+3427 with other pulsars is beneficial for determining the type of companion star in this new binary. Most binary MSPs in our Galaxy are highly recycled ($P \leqslant 10$ ms) and in highly circularized orbits ($e \leqslant 10^{-3}$). The intermediate spin-period pulsars (10 ms $\leqslant P \leqslant 20$ ms; Camilo et al. 2001; Balakrishnan et al. 2023) tend to have a WD companion (Ferdman et al. 2010), and their orbits have very low eccentricities. The rare DNS systems are survivors from two supernova explosions (Tauris et al. 2017). They tend to have a higher orbital eccentricity in the range of $0.064 \leqslant e \leqslant 0.83$ and orbital periods between $0.1 \leqslant P_b \leqslant 45$ days (Tauris et al. 2017). Their eccentricities are much greater than the high- and intermediate-recycled pulsars.

The spin period of PSR J2150+3427 is consistent with young pulsars, but larger than the recycled NS (old), in DNS systems. In addition, the P_b, e, and $M_{\rm tot}$ of PSR J2150+3427 are consistent with that of the known DNS systems. On the other hand, we also noticed that the M_p–M_c distributions (panel (b) in Figure 3) of PSR J2150+3427 are consistent with three NS–WD systems (PSRs J1141−6545, J2222−0137, B2303+46). This suggests that PSR J2150+3427 may possess a massive WD companion. To better determine whether it belongs to a DNS or a massive NS–WD system, we use the system mass ratio q ($q = M_p/M_c$) and define an orbital factor Q ($Q = P_b/e$ day) to compare PSR 2150+3424 with known DNS and NS–WD systems.

The Q–q diagram for PSR J2150+3427 and the known DNS systems are shown in Figure 3. As shown in panel (c), the Q-factor of the known DNS system is less than 37 days, and q is between 0.91 and 1.33 (∼1). Assuming that the orbital inclination is $i = 90°$ and 60°, and that J2150+3427 has $q = 1.54(5)$ and $q = 1.20(4)$, respectively, the Q of PSR J2150+3427 is given by ∼17.61 days. Obviously, the Q and q values for PSR J2150+3427 are in good agreement with the DNS systems but differ significantly from most NS–WD systems. In the Q–q diagram, the distribution of this pulsar is also consistent with the location of PSRs J1141−6545 and B2303+46, which implies that PSR J2150+3427 may have a massive WD companion.

The noticeable differences between PSR J2150+3427 and J2222−0137 are the eccentricity, age, and spin period. PSR J2222−0137 has a smaller period ($P \sim 0.032$ s), more circularized orbit ($e \sim 3.8 \times 10^{-4}$), and younger age, which could distinguish it from the DNSs in the Q–q diagram. However, PSR J2150+3427 is an older pulsar in an eccentric orbit, which suggests that it is different from recycled NS–WD systems (e.g., PSR J2222−0137).

PSRs J1141−6545 and B2303+46 are young nonrecycled pulsars (Davies et al. 2002), and their companions are confirmed as WDs, which appear to have formed before the NS (van Kerkwijk & Kulkarni 1999; Kaspi et al. 2000; Davies et al. 2002). Their commonality with PSR J2150+3427 means that they cannot be distinguished from the DNSs through the companion star mass and orbital parameters. Especially when comparing B2303+46 with J2150+3427, they show very similar period, orbital eccentricity, orbital period, and magnetic field. However, the characteristic age are different by about 2 orders of magnitude. Furthermore, the difference in characteristic age between PSRs J2150+3427 and J1141−6545 is about 3 orders of magnitude. This suggests that PSR J2150+3427 does not belong to the younger nonrecycled pulsars, unless it is very old.

Known NS–WD systems with orbital periods of $9 \sim 11$ days have $e < 6.6 \times 10^{-3}$, $P < 30$ ms (MSPs), and characteristic ages between 58 Myr and 45 Gyr (mean value 9.3 Gyr). They have undergone a recycled process. In comparison, PSR J2150+3427 is also an old pulsar (2.86 Gyr) but not significantly recycled ($P \sim 0.654$ s and $e \sim 0.601$). Based on the fact that the companion star cannot provide enough mass for the recycling process, PSR J2150+3427's companion star is probably an NS. Moreover, the consistency of $M_{\rm tot}$, Q, and q suggests that PSR J2150+3427 is likely belong to a DNS system. The DNS evolution described by Tauris et al. (2017) may be applicable to PSR J2150+3427.

In a DNS system, the first NS born is the A star (recycled), and the last one born is the B star (nonrecycled). As described by Tauris et al. (2017), the spin period of recycled pulsars as a rough function of P_b in all the observed Galactic disk DNS systems follows the relation:

$$P = 44 \text{ ms } (P_b/\text{day})^{0.26}. \quad (5)$$

The P of PSR J2150+3427 is different from the predicted value (∼81.27 ms) for recycled DNSs but similar to nonrecycled DNS pulsars (B star), which suggests that it is likely to be an aged B star. Like most DNS systems, we did not detect any signals from the second NS. One possible reason is that its beam of radiation does not sweep pass the Earth. Therefore, we cannot absolutely confirm whether it is an A star or B star.

There are observations for a potential companion of PSR J2150+3427 in Gaia Data Release 3 Part 1 (Gaia Collaboration 2022) with an offset of 0.″0118 from the pulsar's position. The source ID is 1948939718066589952, and the mean magnitude of the source in the G band is 20 mag. It indicates that better telescopes are needed to obtain more information on its distance, temperature, proper motion, and so on. This source could be a foreground star or a background star.

Using the equation described by Bergeron et al. (1995) and Ruiz et al. (1995), the visual magnitude (m) of a WD can be estimated by the following relation:

$$m = -2.5 \log f_\lambda - 21.1158, \quad (6)$$

where

$$f_\lambda = 4\pi (R/d)^2 H_\lambda \quad (7)$$

and R is the radius of the WD, d is the distance, H_λ is the monochromatic Eddington flux (in units of ergs cm^{-2} s^{-1} Hz^{-1} str^{-1}), whose value is given in Table 1 of Bergeron et al. (1995). For B2303+46s WD companion, at a DM distance of 4.3 kpc and for a cooling timescale of ∼30 Myr, a 1.3 $M_\odot$ WD counterpart would have $m \sim 25.8$. This value is close to the measured value of 26.60(9) mag in the B band (van Kerkwijk & Kulkarni 1999). For PSR J2150+3427, we assume that the companion has an age close to the characteristic age of the pulsar (∼2.88 Gyr). When using a DM distance from the YMW16 model (4.77 kpc) and a WD mass of 1.02 $M_\odot$ ($i = 90°$), the magnitude is estimated to be $m \sim 28.5$. At the DM distance given by the NE2000 model, the value is estimated to be $m \sim 27.5$. When using a WD mass of 1.18 $M_\odot$

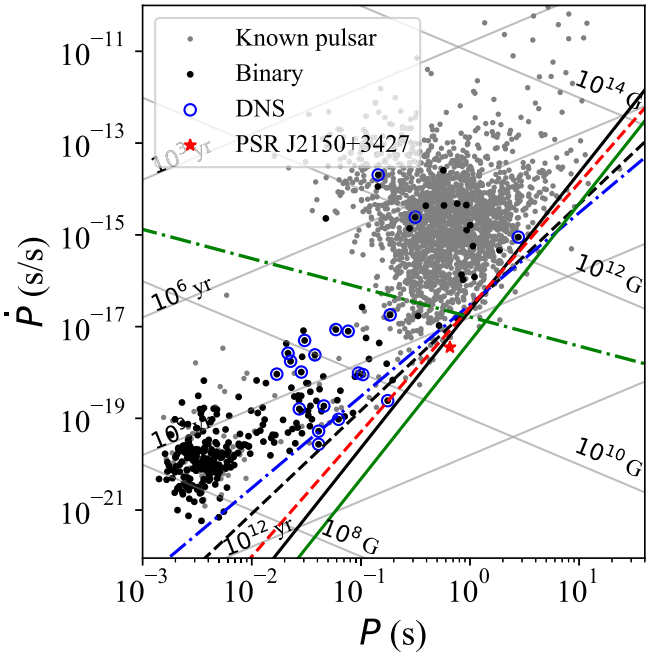

Figure 4. The P–$\dot{P}$ diagram of the known pulsars, including PSR J2150+3427. The binary pulsars are indicated in black, DNS systems are represented by the blue circles, and PSR J2150+3427 is indicated by the red star. The blue and green dashed–dotted lines are the death lines predicted by the CR-induced space-charged-limited flow (SCLF) models and the inverse Compton scattering-induced SCLF model, respectively (Zhang et al. 2000). The blue dashed line is the death line predicted by the CR-induced vacuum gap model proposed by Zhang et al. (2000). The black line is a typical death line predicted by CR from the vacuum gap model (Ruderman & Sutherland 1975). The black dashed line is modeled by Equation (9) of Chen & Ruderman (1993). The green solid line is the death line model from Zhou et al. (2017).

($i = 60°$), the estimations are $m \sim 29.1$ and $m \sim 28.1$, respectively. The companion of PSR J2150+3427 is more difficult to observe than B2303+46. The pulsar could be nonrecycled and just very old. If that were the case the companion could be a WD.

4.3. The Pulsar Death Line

Currently, PSR J2150+3427 is a pulsar with the lowest spin-down luminosity in binary systems (PSRCAT version 1.69). The rotational parameters of PSR J2150+3427 imply that it has an $\dot{E} = 5.10(10) \times 10^{29}$ erg s^{-1} and it is an old pulsar ($\tau_c = 2.86(6) \times 10^9$ yr). This places it below the typical death line (black line in the P–$\dot{P}$ diagram), shown in Figure 4, where a few pulsars are known. Traditionally, radio-quiet pulsars are supposed to be located under the death line. Various death lines are presented in the P–$\dot{P}$ diagram by earlier investigators. In Figure 4, the black line is a typical death line based on curvature radiation (CR) in the vacuum gap (V) model, as proposed by Ruderman & Sutherland (1975). So far, 55 pulsars (PSRCAT version 1.69) have been found below this line, meaning that the models cannot explain the origin of radio emission from these sources. Chen & Ruderman (1993) defined the region with two death lines forming the pulsar death valley (Equations (6) and (9) in their article). As shown in Figure 4, the black dashed line is a death line modeled by Equation (9) proposed by Chen & Ruderman (1993). About 38 pulsars are below this line. Neither the typical death line nor the death valley can explain the emission of PSR J2150+3427.

We have also explored the death line model of Zhang et al. (2000) to explain PSR J2150+3427. In Figure 4, the death lines as predicted by the CR-induced space-charged-limited flow (SCLF) model and by the inverse Compton scattering (ICS)-induced SCLF model are indicated by the blue and green dashed–dotted lines, respectively. The blue dashed line is the death line predicted by the CR-induced vacuum gap model proposed by Zhang et al. (2000). These two models cannot explain the radio radiation in PSR J2150+3427. We also noticed that the CR-V and ICS-V models of Zhang et al. (2000) cannot explain PSR J2150+3427. This suggests that the death line models need improvement.

As described by Zhou et al. (2017), different equations of state (EOS) for a pulsar result in different death lines. The mass of PSR J2150+3427 is $<1.67\,M_\odot$. The moment of inertia and the radius for an NS of a specific mass, together with the associated EOSs, are given in Table 1 by Zhou et al. (2017). Like Zhou et al. (2017), we adopt the typical potential drop $\Delta V = 10^{12}$ V in the polar cap accelerating region. At the inclination angle of 90°, the death line model with EOS named wwf1 in Zhou et al. (2017) can explain the radio luminosity of PSR J2150+3427 (the green solid line in Figure 4).

Szary et al. (2014) proposed an alternative explanation for the pulsar emission cessation process. They suggest that radio emission may be assumed to have a maximum possible efficiency ($\xi_{\rm max} \equiv L/\dot{E} = 0.01$). Here, L is the radio luminosity, which can be obtained from Equation (2) of Szary et al. (2014). Assuming a spectral index of −1.6 (Lorimer et al. 1995), the radio efficiency of PSR J2150+3427 is ∼0.064 and 0.025, based on the distances predict from the NE2001 and the YMW16 models, respectively. The radio efficiency is greater than the maximum possible efficiency proposed by Szary et al. (2014). Based on the maximum radio efficiency of pulsars ($\xi_{\rm max} \equiv L/\dot{E} = 0.01$; Szary et al. 2014) and the sensitivity of the radio telescope, Wu et al. (2020) proposed an "observation-limit line" ($\dot{E}_{\rm min} = L/\xi_{\rm max}$) to explain low $\dot{E}$ pulsars discovered in the "grave yard" in the P–$\dot{P}$ diagram. According to the sensitivity of FAST ($S_{\rm min} = 3.1\ \mu$s; Nan et al. 2011), the possible minimum $\dot{E}$ ("observation-limit line") at the same distance as PSR J2150+3427 is $\sim 5.2 \times 10^{28}$ erg s^{-1}. We noticed that the $\dot{E}$ of PSR J2150+3427 is greater than $\dot{E}_{\rm min}$, which suggests that this "observation-limit line" can explain its flux density luminosity.

5. Conclusions and Future Work

In this paper, we have reported the discovery and timing campaign of PSR J2150+3427. It is a 654 ms binary pulsar with an eccentric orbit ($e = 0.601$) of 10.592 days around a possible NS. Using our 2 yr data set, we also measured the rate of periastron advance, whose value suggests that the total mass of PSR J2150+3427 is consistent with the known DNSs in our Galaxy. Based on the orbital factor and mass ratio, PSR J2150+3427's companion star is probably an NS. Currently, it is the known pulsar with the smallest $\dot{E}$ in a binary system outside of globular clusters (PSRCAT version 1.69).

The $\dot{\omega}$ of all known DNSs are in the range of 0.00078(4) to 25.6(3) deg yr^{-1} and have an average value of 5.4(3) deg yr^{-1}. The $\dot{\omega}$ of PSR J2150+3427 is in accordance with that of the DNS population. Continued follow-up observations may determine the masses of PSR J2150+3427 and its companion via detection of more relativistic effects (PK parameters). One of these parameters, known as the Shapiro delay, can be

observed in highly inclined (nearly edge-on) DNS systems (Shapiro 1964). As described by Freire & Wex (2010), a new PK parameter h_3 follows

$$h_3 = r\,\varsigma^3 = r\left(\frac{s}{1+\sqrt{1-s^2}}\right)^3 = T_\odot\, m_c\left(\frac{\sin i}{1+|\cos i|}\right)^3, \tag{8}$$

where h_3 is the "orthometric amplitude parameter" of the Shapiro delay, r is the "range" of Shapiro delay, ς is the "orthometric ratio" parameter expressed in the ratio of the amplitude to the successive harmonics of the Shapiro delay, and s is the "shape" of Shapiro delay. For an inclination angle of 60°, the value of h_3 would be 1.2 μs, which is probably undetectable given our EQUAD of 9 μs. If the Shapiro delay cannot be detected, measuring the mass of the companion would require using the Einstein delay, which will take decades.

Acknowledgments

This is work is supported by the National Key Research and Development Program of China (No. 2022YFC2205203), the National Natural Science Foundation of China grant (Nos. 12288102, 12041303, 12041304, 12273100, T2241020), and the Major Science and Technology Program of Xinjiang Uygur Autonomous Region (Nos. 2022A03013-2, 2022A03013-3, 2022A03013-4). D.L. is supported by the 2020 project of Xinjiang Uygur autonomous region of China for flexibly fetching in upscale talents. P.W. acknowledges support from the National Natural Science Foundation of China under grant U2031117, the Youth Innovation Promotion Association CAS (id. 2021055), CAS Project for Young Scientists in Basic Reasearch (grant YSBR-006), and the Cultivation Project for FAST Scientific Payoff and Research Achievement of CAMS-CAS. W.W.Z. is supported by National SKA Program of China No. 2020SKA0120200, and National Nature Science Foundation grant No. 11873067. S.J.D. is supported by Guizhou Provincial Science and Technology Foundation (Nos. ZK [2022]304) and Foundation of Education Bureau of Guizhou Province, China (grant No. KY (2020) 003). J.M.Y. is Sponsored by Natural Science Foundation of Xinjiang Uygur Autonomous Region (No. 2022D01D85), the Tianshan Talent project and the CAS Project for Young Scientists in Basic Research (grant YSBR-063). This work made use of the data from FAST (Five-hundred-meter Aperture Spherical radio Telescope). FAST is a Chinese national mega-science facility, operated by National Astronomical Observatories, Chinese Academy of Sciences. We would like to thank the FAST CRAFTS group and XAO pulsar group for data provide and helpful suggestions that led to significant improvement in our study.

ORCID iDs

N. Wang https://orcid.org/0000-0002-9786-8548
J. P. Yuan https://orcid.org/0000-0002-5381-6498
D. Li https://orcid.org/0000-0003-3010-7661
P. Wang https://orcid.org/0000-0002-3386-7159
M. Y. Xue https://orcid.org/0000-0001-8018-1830
W. W. Zhu https://orcid.org/0000-0001-5105-4058
C. C. Miao https://orcid.org/0000-0002-9441-2190
W. M. Yan https://orcid.org/0000-0002-7662-3875
J. B. Wang https://orcid.org/0000-0001-9782-1603
J. M. Yao https://orcid.org/0000-0002-4997-045X
S. Q. Wang https://orcid.org/0000-0003-4498-6070
F. F. Kou https://orcid.org/0000-0002-0069-831X
D. Zhao https://orcid.org/0009-0007-8062-1454
Y. Feng https://orcid.org/0000-0002-0475-7479
L. Q. Meng https://orcid.org/0000-0002-2885-568X
M. Yuan https://orcid.org/0000-0003-1874-0800
C. H. Niu https://orcid.org/0000-0001-6651-7799
J. R. Niu https://orcid.org/0000-0001-8065-4191
L. Qian https://orcid.org/0000-0003-0597-0957
S. Wang https://orcid.org/0000-0002-1570-7485
Y. L. Yue https://orcid.org/0000-0003-4415-2148
X. Zhou https://orcid.org/0000-0003-4686-5977
L. Zhang https://orcid.org/0000-0001-8539-4237

References

Agazie, G. Y., Mingyar, M. G., McLaughlin, M. A., et al. 2021, ApJ, 922, 35
Alpar, M. A., Cheng, A. F., Ruderman, M. A., & Shaham, J. 1982, Natur, 300, 728
Balakrishnan, V., Freire, P. C. C., Ransom, S. M., et al. 2023, ApJL, 942, L35
Bergeron, P., Wesemael, F., & Beauchamp, A. 1995, PASP, 107, 1047
Bernadich, M. C. I., Balakrishnan, V., Barr, E., et al. 2023, A&A, 678, A187
Bhattacharya, D., & van den Heuvel, E. P. J. 1991, PhR, 203, 1
Bhattacharya, D., Wijers, R. A. M. J., Hartman, J. W., & Verbunt, F. 1992, A&A, 254, 198
Cameron, A. D., Li, D., Hobbs, G., et al. 2020, MNRAS, 495, 3515
Camilo, F., Lyne, A. G., Manchester, R. N., et al. 2001, ApJL, 548, L187
Cantiello, M., Yoon, S. C., Langer, N., & Livio, M. 2007, A&A, 465, L29
Chen, K., & Ruderman, M. 1993, ApJ, 402, 264
Cordes, J. M., & Lazio, T. J. W. 2002, arXiv:astro-ph/0207156
Corongiu, A., Kramer, M., Stappers, B. W., et al. 2007, A&A, 462, 703
Cruces, M., Champion, D. J., Li, D., et al. 2021, MNRAS, 508, 300
Damour, T., & Deruelle, N. 1985, AIHPA, 43, 107
Damour, T., & Deruelle, N. 1986, AIHPA, 44, 263
Davies, M. B., Ritter, H., & King, A. 2002, MNRAS, 335, 369
Deller, A. T., Goss, W. M., Brisken, W. F., et al. 2019, ApJ, 875, 100
Edwards, R. T., Hobbs, G. B., & Manchester, R. N. 2006, MNRAS, 372, 1549
Eichler, D., Livio, M., Piran, T., & Schramm, D. N. 1989, Natur, 340, 126
Ferdman, R. D., Stairs, I. H., Kramer, M., et al. 2010, ApJ, 711, 764
Ferdman, R. D., Stairs, I. H., Kramer, M., et al. 2014, MNRAS, 443, 2183
Freire, P. C. C., & Wex, N. 2010, MNRAS, 409, 199
Gaia Collaboration 2022, yCat, I/355
Hobbs, G. B., Edwards, R. T., & Manchester, R. N. 2006, MNRAS, 369, 655
Hotan, A. W., van Straten, W., & Manchester, R. N. 2004, PASA, 21, 302
Jiang, P., Tang, N.-Y., Hou, L.-G., et al. 2020, RAA, 20, 064
Kaspi, V. M., Lyne, A. G., Manchester, R. N., et al. 2000, ApJ, 543, 321
Kramer, M., Stairs, I. H., Manchester, R. N., et al. 2021, PhRvX, 11, 041050
Lentati, L., Alexander, P., Hobson, M. P., et al. 2014, MNRAS, 437, 3004
Lewin, W. H. G., & van der Klis, M. 2006, Compact Stellar X-Ray Sources, Vol. 39 (Cambridge: Cambridge Univ. Press)
Li, D., Wang, P., Qian, L., et al. 2018, IMMag, 19, 112
Lorimer, D. R. 2008, LRR, 11, 8
Lorimer, D. R., & Kramer, M. 2004, Handbook of Pulsar Astronomy, Vol. 4 (Cambridge: Cambridge Univ. Press)
Lorimer, D. R., Yates, J. A., Lyne, A. G., & Gould, D. M. 1995, MNRAS, 273, 411
Manchester, R. N., Hobbs, G. B., Teoh, A., & Hobbs, M. 2005, AJ, 129, 1993
Martinez, J. G., Stovall, K., Freire, P. C. C., et al. 2017, ApJL, 851, L29
Miao, C. C., Zhu, W. W., Li, D., et al. 2023, MNRAS, 518, 1672
Nan, R., Li, D., Jin, C., et al. 2011, IJMPD, 20, 989
Özel, F., & Freire, P. 2016, ARA&A, 54, 401
Phinney, E. S. 1992, RSPTA, 341, 39
Pol, N., McLaughlin, M., & Lorimer, D. R. 2019, ApJ, 870, 71
Qian, L., Yao, R., Sun, J., et al. 2020, Innov, 1, 100053
Ruderman, M. A., & Sutherland, P. G. 1975, ApJ, 196, 51
Ruiz, M. T., Bergeron, P., Leggett, S. K., & Anguita, C. 1995, ApJL, 455, L159
Sengar, R., Balakrishnan, V., Stevenson, S., et al. 2022, MNRAS, 512, 5782
Shapiro, I. I. 1964, PhRvL, 13, 789
Shklovskii, I. S. 1970, SvA, 13, 562

Swiggum, J. K., Pleunis, Z., Parent, E., et al. 2023, ApJ, 944, 154
Szary, A., Zhang, B., Melikidze, G. I., Gil, J., & Xu, R.-X. 2014, ApJ, 784, 59
Tauris, T. M., Kramer, M., Freire, P. C. C., et al. 2017, ApJ, 846, 170
Tauris, T. M., & van den Heuvel, E. P. J. 2006, in Formation and evolution of compact stellar X-ray source, ed. W. Lewin & M. van der Klis, Vol. 39 (Cambridge: Cambridge Univ. Press), 623
Taylor, J. H., & Weisberg, J. M. 1982, ApJ, 253, 908
van Kerkwijk, M. H., & Kulkarni, S. R. 1999, ApJL, 516, L25
van Straten, W., & Bailes, M. 2011, PASA, 28, 1
van Straten, W., Demorest, P., Khoo, J., et al., 2011 PSRCHIVE: Development Library for the Analysis of Pulsar Astronomical Data, Astrophysics Source Code Library, ascl:1105.014
Wex, N. 2014, arXiv:1402.5594
Wu, Q. D., Yuan, J. P., Wang, N., et al. 2023, MNRAS, 522, 5152
Wu, Q.-D., Zhi, Q.-J., Zhang, C.-M., Wang, D.-H., & Ye, C.-Q. 2020, RAA, 20, 188
Yao, J. M., Manchester, R. N., & Wang, N. 2017, ApJ, 835, 29
Zhang, B., Harding, A. K., & Muslimov, A. G. 2000, ApJL, 531, L135
Zhou, X., Tong, H., Zhu, C., & Wang, N. 2017, MNRAS, 472, 2403